

Article

Unlocking the Hidden Genetic Diversity of Varicosaviruses, the Neglected Plant Rhabdoviruses

Nicolas Bejerman^{1,2,*} , Ralf G. Dietzgen^{3,*}  and Humberto Debat^{1,2,*} 

- ¹ Instituto de Patología Vegetal, Centro de Investigaciones Agropecuarias, Instituto Nacional de Tecnología Agropecuaria (IPAVE—CIAP—INTA), Camino 60 Cuadras Km 5.5, Córdoba X5020ICA, Argentina
- ² Consejo Nacional de Investigaciones Científicas y Técnicas, Unidad de Fitopatología y Modelización Agrícola, Camino 60 Cuadras Km 5.5, Córdoba X5020ICA, Argentina
- ³ Queensland Alliance for Agriculture and Food Innovation, The University of Queensland, St. Lucia, QLD 4072, Australia
- * Correspondence: bejerman.nicolas@inta.gob.ar (N.B.); r.dietzgen@uq.edu.au (R.G.D.); debat.humberto@inta.gob.ar (H.D.)

Abstract: The genus *Varicosavirus* is one of six genera of plant-infecting rhabdoviruses. Varicosaviruses have non-enveloped, flexuous, rod-shaped virions and a negative-sense, single-stranded RNA genome. A distinguishing feature of varicosaviruses, which is shared with dichorhviruses, is a bi-segmented genome. Before 2017, a sole varicosavirus was known and characterized, and then two more varicosaviruses were identified through high-throughput sequencing in 2017 and 2018. More recently, the number of known varicosaviruses has substantially increased in concert with the extensive use of high-throughput sequencing platforms and data mining approaches. The novel varicosaviruses have revealed not only sequence diversity, but also plasticity in terms of genome architecture, including a virus with a tentatively unsegmented genome. Here, we report the discovery of 45 novel varicosavirus genomes which were identified in publicly available metatranscriptomic data. The identification, assembly, and curation of the raw Sequence Read Archive reads has resulted in 39 viral genome sequences with full-length coding regions and 6 with nearly complete coding regions. The highlights of the obtained sequences include eight varicosaviruses with unsegmented genomes, which are linked to a phylogenetic clade associated with gymnosperms. These findings have resulted in the most complete phylogeny of varicosaviruses to date and shed new light on the phylogenetic relationships and evolutionary landscape of this group of plant rhabdoviruses. Thus, the extensive use of sequence data mining for virus discovery has allowed us to unlock of the hidden genetic diversity of varicosaviruses, the largely neglected plant rhabdoviruses.

Keywords: plant rhabdovirus; varicosaviruses; genome architecture; virus taxonomy; metatranscriptomics



Citation: Bejerman, N.; Dietzgen, R.G.; Debat, H. Unlocking the Hidden Genetic Diversity of Varicosaviruses, the Neglected Plant Rhabdoviruses. *Pathogens* **2022**, *11*, 1127. <https://doi.org/10.3390/pathogens11101127>

Academic Editor: Lawrence S. Young

Received: 20 September 2022

Accepted: 27 September 2022

Published: 29 September 2022

Publisher's Note: MDPI stays neutral with regard to jurisdictional claims in published maps and institutional affiliations.



Copyright: © 2022 by the authors. Licensee MDPI, Basel, Switzerland. This article is an open access article distributed under the terms and conditions of the Creative Commons Attribution (CC BY) license (<https://creativecommons.org/licenses/by/4.0/>).

1. Introduction

A recently discovered huge number of diverse viruses has revealed the complexities of the evolutionary landscape of replicating entities and the challenges associated with their classification [1], leading to the first comprehensive proposal of the virus world megataxonomy [2]. Nevertheless, a minuscule portion, likely a small fraction of one percent, of the virosphere has been characterized so far [3]. Therefore, we have a limited knowledge of the vast world virome, with its remarkable diversity, that includes every potential host organism assessed so far [4–6]. Data mining of publicly available transcriptome datasets has become an efficient and inexpensive strategy to unlock the diversity of the plant virosphere [5]. Data-driven virus discovery relies on the vast number of available datasets on the Sequence Read Archive (SRA) of the National Center for Biotechnology Information (NCBI). This resource, which is growing at an exceptional rate and includes data of a large and diverse number of organisms, represents a substantial fraction of species that

populate our planet, which makes the SRA database an invaluable source to identify novel viruses [7].

Varicosavirus is one of the six genera that are comprised of plant rhabdoviruses (family *Rhabdoviridae*, subfamily *Betarhabdovirinae*), and its members are thought to have a negative-sense, single-stranded, bi-segmented RNA genome [8]. Nevertheless, recently, we described the first apparently unsegmented varicosavirus [9]. In those varicosaviruses with segmented genomes, RNA 1 consists of one to two genes, with one of those encoding the RNA-dependent RNA polymerase L, while RNA 2 consists of three to five genes, with the first open reading frame (ORF) encoding a nucleocapsid protein (N) [8,10]. On the other hand, the only unsegmented varicosavirus described so far has five ORFs, in the order: 3'-N-Protein 2-Protein 3-Protein 4-L-5' [9]. Varicosaviruses appear to have a diverse host range that includes dicots, monocots, gymnosperms, ferns, and liverworts [6,9]. The vector of a sole member, lettuce big vein-associated virus (LBVaV), has been characterized, which is the chytrid fungus *Olpidium* spp. [11].

Until 2017, LBVaV was the only identified and extensively characterized varicosavirus [12–14], and then, in 2017 and 2018, two novel varicosaviruses were identified through high-throughput sequencing (HTS) [15,16]. However, in 2021 and 2022, there was a five-fold increase in the number of reported varicosaviruses, with 12 out of 15 discovered through data mining of publicly available transcriptome datasets [6,9,17,18], while the other three were identified using HTS [19–21] (Supplementary Figure S1). Nevertheless, only some minor biological aspects, such as mechanical transmissibility, of some of these members were further characterized [15,20]. Therefore, varicosaviruses are, by far, the least-studied plant rhabdoviruses, and many aspects of their epidemiology remain elusive. In terms of genetic diversity, before this study, while greatly expanded by recent works, the *Varicosavirus* genus includes only three accepted species and 15 tentative members.

In this study, we identified 45 novel varicosaviruses by analyzing publicly available metatranscriptomic data. Thus, the extensive use of data mining for virus discovery has allowed us to unlock some of the hidden diversity of varicosaviruses, the much-neglected plant rhabdoviruses.

2. Material and Methods

2.1. Identification of Plant Rhabdovirus Sequences from Public Plant RNA-seq Datasets

Three strategies were used to detect varicosavirus sequences: (1) Amino acid sequences corresponding to the nucleocapsid and polymerase proteins of known varicosaviruses were used as queries in tBlastn searches with the parameters word size = 6, expected threshold = 10, and scoring matrix = BLOSUM62, against the Viridiplantae (taxid: 33090) Transcriptome Shotgun Assembly (TSA) sequence databases. The obtained hits were manually explored and based on percentage identity, query coverage, and E-value ($>1 \times 10^{-5}$) and shortlisted as likely corresponding to novel virus transcripts, which were then further analyzed. (2) Raw sequence data corresponding to the SRA database associated with the 1K study [22] were explored for varicosa-like virus sequences. (3) The Serratus database was explored, employing the serratus explorer tool [5], and using as queries the sequences of LBVaV, red clover varicosavirus, and black grass varicosavirus. Those SRA libraries that matched the query sequences (alignment identity > 45%; score > 10) were further explored in detail.

2.2. Sequence Assembly and Identification

The nucleotide (nt) raw sequence reads from each SRA experiment, which are associated with different NCBI bioprojects (Table 1), were downloaded and pre-processed by trimming and filtering with the Trimmomatic tool as implemented in <http://www.usadellab.org/cms/?page=trimmomatic> (accessed on 19 August 2022). The resulting reads were assembled de novo with rnaSPAdes using standard parameters on the Galaxy.org server. The transcripts obtained from the de novo transcriptome assembly were subjected to bulk local BLASTX searches (E-value $< 1 \times 10^{-5}$) against a collection of varicosavirus protein se-

quences available at [https://www.ncbi.nlm.nih.gov/protein?term=txid140295\[Organism\]](https://www.ncbi.nlm.nih.gov/protein?term=txid140295[Organism]) (accessed on 19 August 2022). The resulting viral sequence hits of each bioproject were visually explored. Tentative virus-like contigs were curated (extended or confirmed) by iteratively mapping each SRA library's filtered reads. This strategy used BLAST/nhmmr to extract a subset of reads related to the query contig and used the retrieved reads to extend the contig and then repeated the process iteratively using the extended sequence as query. The extended and polished transcripts were reassembled using the Geneious v8.1.9 (Biomatters Ltd., San Diego, CA, USA) alignment tool with high sensitivity parameters. Bowtie2, available at <http://bowtie-bio.sourceforge.net/bowtie2/index.shtml> (accessed on 26 September 2022), was used with standard parameters for filtered read mapping to calculate the mean coverage of each assembled virus sequence.

Table 1. Summary of the novel varicosaviruses identified from the plant RNA-seq data available in the NCBI database. The acronyms of the best hits are listed in Supplementary Table S1.

Plant Host	Taxa/Family	Virus Name/Abbreviation	Bioproject ID/Data Citation	Segment/Coverage	Length (nt)	Accession Number	Protein ID	Length (aa)	Highest Scoring Virus-Protein/E-Value/Query Coverage%/Identity% (Blast P)
Trojan fir (<i>Abies nordmannia</i>)	Gymnosperm/ <i>Pinaceae</i>	Abies virus 1/ AbiV1	PRJNA387306/ University of Connecticut, USA	RNA1/30.97X	11,287	BK061731	N	430	PiFleV1-N/9e-130/87/50.79
							2	420	PiFleV1-P2/2e-18/57/28.05
							3	317	PiFleV1-P3/2e-103/97/47.44
							4	163	no hits
							L	2050	PiFleV1-L/0.0/98/52.68
Dwarf mistletoe (<i>Arceuthobium sichuanense</i>)	dicot/ <i>Santalaceae</i>	Arceuthobium virus 8/ ArcV8	PRJNA307530/ [23]	RNA1/9.31X RNA2/72.35X	6628 4149	BK061732 BK061733	L	2013	ASaV2-L/0.0/98/100
							N	369	ZaVV1-N/1e-34/91/28.36
							2	453	no hits
							3	159	no hits
Bei Wu Tou (<i>Aconitum kusnezoffii</i>)	dicot/ <i>Ranunculaceae</i>	Aconitum virus 1/ AcoV1	PRJNA670255/ [24]	RNA1/10.16X RNA2/105.03X	6483 5561	BK061734 BK061735	L	2000	ZaVV1-L/0.0-97/61.18
							N	424	ZaVV1-N/2e-115/99/43.82
							2	329	VVV-P2/4e-36/80/32.13
							3	311	ZaVV1-P3/5e-105/85/54.51
							4	204	VVV-P4/1e-27/87/33.33
5	297	VVV-P5/5e-17/92/26.18							
Catkin yew (<i>Amentotaxus argotaenia</i>)	Gymnosperm/ <i>Cephalotaxaceae</i>	Amentotaxus virus 1/ AmeV1	PRJNA498605/ [25]	RNA1/109.96X	10,965	BK061736	N	391	ASaV2-N/3e-111/94/45.95
							2	431	PiFleV1-P2/1e-06/55/26.98
							3	314	ASaV2-P3/4e-83/94/43.42
							4	187	no hits
							L	2062	PiFleV1-L/0.0/99/46.16
Common windgrass (<i>Apera spica-venti</i>)	monocot/ <i>Poaceae</i>	Apera virus 1/ ApeV1	PRJNA356380/ [26]	RNA1/11.98X RNA2/110.50X	6516 6552	BK061737 BK061738	L	2027	MelRoV1-L/0.0/98/52.12
							N	447	MelRoV1-N/2e-69/82/34.57
							2	363	MelRoV1-P2/4e-17/75/26.37
							3	298	MelRoV1-P3/2e-80/97/41.25
							4	196	no hits
5	444	no hits							
Lace plant (<i>Aponogeton madagascariensis</i>)	monocot/ <i>Aponogetonaceae</i>	Aponogeton virus 1/ ApoV1	PRJNA591467/ [27]	RNA1/36.42X RNA2/81.25X	6678 5628	BK061739 BK061740	L	2022	BrRV1-L/0.0/98/52.7
							N	435	BrRV1-N/7e-81/88/37
							2	454	no hits
							3	300	TfVV-P3/2e-45/96/34
4	174	BrRV1-P3/0.003/73/25							
Wormwood (<i>Artemisia absinthium</i>)	dicot/ <i>Asteraceae</i>	Artemisia virus 1/ ArtV1	PRJNA371565/ [28]	RNA1/33.06X RNA2/50.30X	7373 4497	BK061741 BK061742	L	2020	BrRV1-L/0.0/98/49.18
							N	453	BrRV1-N/3e-45/76/28.90
							2	494	no hits
3	174	no hits							
Common milkweed (<i>Asclepias syriaca</i>)	dicot/ <i>Apocynaceae</i>	<i>Asclepias syriaca</i> virus 3 AscSyV3	PRJNA210776/ [29]	RNA1/37.86X RNA2/138.94X	6506 6280	BK061743 BK061744	L	2021	TfVV-L/0.0/94/42.62
							N	453	TfVV-N/3e-39/78/32.13
							2	370	no hits
							3	286	TfVV-P3/73-32/78/29.26
							4	160	no hits
5	393	no hits							
Beautiful tree fern (<i>Asplenium loricatum</i>)	<i>Polypodiophyta</i> / <i>Aspleniaceae</i>	Asplenium virus 1/ AspV1	PRJNA281136/ [30]	RNA1/4.51X RNA2/8.91X	6287 * 4371 *	BK061745 BK061746	L	1957 *	TfVV-L/0.0/98/43.81
							N	396	TfVV-N/2e-79/90/37.82
							2	490	no hits
							3	294	TfVV-P3/1e-45/87/33.33
4	127 *	no hits							

Table 1. Cont.

Plant Host	Taxa/Family	Virus Name/Abbreviation	Bioproject ID/Data Citation	Segment/Coverage	Length (nt)	Accession Number	Protein ID	Length (aa)	Highest Scoring Virus-Protein/E-Value/Query Coverage%/Identity% (Blast P)
Shortpod mustard (<i>Brassica incana</i>) ₁	dicot/ <i>Brassicaceae</i>	Brassica virus 2_Inc/ BrV2_Inc	PRJNA428769/ [31]	RNA1/11.89X RNA2/14.63X	6316 5616	BK061747 BK061748	L	2032	TfVV-L/0.0/99/41.86
							N	591	LoPV1-N/1e-31/58/27.93
							2	459	no hits
							3	282	TfVV-P3/9e-33/91/29.32
4	141	no hits							
Indian mustard (<i>Brassica juncea</i> var. <i>rugosa</i>)	dicot/ <i>Brassicaceae</i>	Brassica virus 2_Jun/ BrV2_Jun	PRJNA290942/ [32]	RNA1/80.91X RNA2/950.63X	6316 5537	BK061749 BK061750	L	2032	TfVV-L/0.0/99/41.57
							N	591	LoPV1-N/1e-31/58/27.65
							2	459	no hits
							3	282	TfVV-P3/1e-32/91/29.32
4	141	no hits							
Chinese kale (<i>Brassica oleracea</i> var. <i>alboglabra</i>)	dicot/ <i>Brassicaceae</i>	Brassica virus 2_Ole/ BrV2_Ole	PRJNA525713/ [33]	RNA1/11.03X RNA2/66.34X	6316 5647	BK061751 BK061752	L	2032	TfVV-L/0.0/99/41.81
							N	591	LoPV1-N/7e-32/58/27.93
							2	459	no hits
							3	282	TfVV-P3/8e-33/91/29.32
4	141	no hits							
Crab-lipped spider orchid (<i>Caladenia plicata</i>)	monocot/ <i>Orchidaceae</i>	Caladenia virus 1/ CalV1	PRJNA384875/ [34]	RNA1/10.51X RNA2/52.44X	6454 5011	BK061755 BK061756	L	2024	BrRV1-L/0.0/98/50.17
							N	449	BrRV1-N/1e-64/97/32.43
							2	468	no hits
							3	293	TfVV-P3/1e-43/86/34.78
4	165	BrRV1-P3/3e-07/61/31.13							
Conflower (<i>Centaurea cyanus</i>)	dicot/ <i>Asteraceae</i>	Centaurea virus 1/ CenV1	PRJNA371565/ [28]	RNA1/63.11X RNA2/159.93X	6789 4567	BK061757 BK061758	L	2019	BrRV1-L/0.0/98/50.50
							N	469	BrRV1-N/6e-48/73/30.72
							2	501	no hits
							3	111	no hits
Chamomile (<i>Chamaemelum nobile</i>)	dicot/ <i>Asteraceae</i>	Chamaemelum virus 1/ ChaV1	PRJNA382469/ [35]	RNA1/21.33X RNA2/234.84X	6670 * 5957	BK061759 BK061760	L	1916 *	VVV-L/0.0/99/58.85
							P6	171	no hits
							N	426	ZaVV1-N/2e-105/95/41.40
							2	346	VVV-P2/2e-19/84/30.28
							3	305	VVV-P3/5e-97/94/49.14
4	255	ZaVV1-P4/3e-05/70/22.1							
5	330	VVV-P5/3e-22/85/29.14							
Melon (<i>Cucumis melo</i>)	dicot/ <i>Cucurbitaceae</i>	Cucumis virus 1/ CucV1	PRJNA381300/ [36]	RNA1/47.79X RNA2/60.05X	6919 5322	BK061761 BK061762	L	2034	AMVV1-L/0.0/99/47.47
							N	341	InPRV-N/4e-77/98/38.71
							2	404	no hits
							3	285	TfVV-P3/1e-46/91/34.21
4	119	no hits							
Chen cypress (<i>Cupressus chengiana</i>)	<i>Gymnosperm/ Cupressaceae</i>	Cupressus virus 1/ CupV1	PRJNA556937/ [37]	RNA1/32.13X	12143	BK061763	N	379	ASaV2-N/2e-106/97/44.59
							2	447	ASaV2-P2/5e-30/67/30.86
							3	313	ASaV2-P3/2e-100/84/53.38
							4	187	no hits
							5	168	no hits
L	2055	PiFleV1-L/0.0/99/48.68							
Tree maidenhair fern (<i>Didymochlaena truncatula</i>)	<i>Polypodiophyta/ Hypodeatiaceae</i>	Didymochlaena virus 1/ DidV1	PRJNA422112/ [38]	RNA1/8.88X RNA2/52.28X	6319 5924	BK061764 BK061765	L	2044	TfVV-L/0.0/100/74.17
							N	386	TfVV-N/0.0/100/72.75
							2	394	TfVV-P2/7e-74/96/40.26
							3	292	TfVV-P3/2e-159/99/70.69
							4	187	TfVV-P4/5e-23/88/30.72
5	374	TfVV-P5/0.0/97/64.11							
Wallflower (<i>Erysimum bastetanum</i>)	dicot/ <i>Brassicaceae</i>	Erysimum virus 1/ EryV1	PRJNA607615/ [39]	RNA1/271.24X RNA2/516.22X	6676 3980	BK061766 BK061767	L	1985	BrRV1-L/0.0/99/62.34
							N	439	BrRV1-N/3e-90/99/33.86
							2	404	no hits
3	172	BrRV1-P3/4e-26/100/31.4							
Liverwort (<i>Frullania orientalis</i>)	<i>Marchantiophyta/ Frullaniaceae</i>	Frullania virus 1/ FruV1	PRJNA505755/ Fairylake Botanical Garden, China	RNA1/11.60X RNA2/8.20X	6458 4363	BK061768 BK061769	L	2033	MgVV-L/0.0/98/54.77
							N	372	MgVV-N/2e-94/97/43.96
							2	336	MgVV-P2/8e-05/56/27.27
							3	289	MgVV-P3/5e-85/89/47.49
4	148	MgVV-P4/4e-05/70/29.81							
Noug (<i>Guizotia abyssinica</i>)	dicot/ <i>Asteraceae</i>	Guizotia virus 1/ GuiV1	PRJNA371565/ [28]	RNA1/153.49X RNA2/1192.66X	6457 4722	BK061770 BK061771	L	2007	MelRoV1-L/0.0/98/60.42
							N	434	MelRoV1-N/3e-103/82/43.96
							2	340	MelRoV1-P2/7e-22/85/24.53
							3	262	no hits
4	307	no hits							
Common velvet grass (<i>Holcus lanatus</i>)	monocot/ <i>Poaceae</i>	Holcus virus 1/ HolV1	PRJEB11654/ [40]	RNA1/19.48X RNA2/29.44X	6571 4397	BK061772 BK061773	L	2031	AMVV1-L/0.0/98/65.12
							N	476	LoPV1-N/8e-132/77/51.23
							2	286	LoPV1-P2/5e-23/56/33.33
							3	211	LoPV1-P2/8e-12/63/29.76
4	161	LoPV1-P3/1e-49/90/51.72							
Oxeye daisy (<i>Leucanthemum vulgare</i>)	dicot/ <i>Asteraceae</i>	Leucanthemum virus 1/ LeuV1	PRJNA371565/ [28]	RNA1/141.76X RNA2/229.85X	6763 4775	BK061774 BK061775	L	2021	BrRV1-L/0.0/98/49.63
							N	448	BrRV1-N/3e-42/71/32.11
							2	520	no hits
3	167	no hits							

Table 1. Cont.

Plant Host	Taxa/Family	Virus Name/Abbreviation	Bioproject ID/Data Citation	Segment/Coverage	Length (nt)	Accession Number	Protein ID	Length (aa)	Highest Scoring Virus-Protein/E-Value/Query Coverage%/Identity% (Blast P)
Downy flax (<i>Linum hirsutum</i>)	dicot/ <i>Linaceae</i>	Linum virus 1/ LinV1	PRJEB21674/ 1000 Plant (1KP) Tran- scriptomes Initiative	RNA1/26.47X RNA2/119.90X	5999 * 6330	BK061776 BK061777	L	1940 *	MelRoV1-L/0.0/94/53.78
							N	450	MelRoV1-/3e-69/82/33.96
							2	463	no hits
							3	313	MelRoV1-P3/7e-81/88/42.39
Sponge gourd (<i>Luffa aegyptiaca</i>)	dicot/ <i>Cucurbitaceae</i>	Luffa virus 1/ LufV1	PRJNA390566/ Mylne, J., The University of Western Australia	RNA1/16.47X RNA2/11.32X	6693 4961	BK061780 BK061781	L	2032	LoPV1-L/0.0/99/49.04
							N	487	InPRV-N/7e-84/86/36.93
							2	366	no hits
							3	286	TfVV-P3/3e-53/81/41.7
Riverbank lupine (<i>Lupinus rivularis</i>)	dicot/ <i>Fabaceae</i>	Lupinus virus 1/ LupV1	PRJNA318864/ [41]	RNA1/14.64X RNA2/97.57X	6688 4042 *	BK061782 BK061783	L	1997	ZaVV1-L/0.0/99/56.91
							N	426	ZaVV1-N/2e-83/99/36.92
							2	497	ZaVV1-P2/3e-14/39/28.99
							3	116 *	no hits
Sweet clover (<i>Melilotus spp</i>)	dicot/ <i>Fabaceae</i>	Melilotus virus 1_Al/1/ MelV1_Al/1	PRJNA647665/ [42]	RNA1/30.69X RNA2/98.21X	6657 3985	BK061784 BK061785	L	2019	RCaVV-L/0.0/99/64.97
							N	430	RCaVV-N/5e-80/93/33.5
							2	393	RCaVV-P2/0.001/42/27.54
Sweet clover (<i>Melilotus spp</i>)	dicot/ <i>Fabaceae</i>	Melilotus virus 1_Off/1/ MelV1_Off	PRJNA751393/ [43]	RNA1/12.15X RNA2/25.36X	6433 3781	BK061786 BK061787	L	2019	RCaVV-L/0.0/99/65.37
							N	430	RCaVV-N/5e-77/91/33.33
							2	399	RCaVV-P2/0.002/42/28.14
Early spider orchid (<i>Ophrys sphegodes</i>)	monocot/ <i>Orchidaceae</i>	Ophrys virus 1/ OphV1	PRJNA574279/ [44]	RNA1/7.72X RNA2/206.15X	6134 * 5036	BK061788 BK061789	L	1988 *	MelRoV1-L/0.0/99/56.95
							N	447	MelRoV1-N/4e-97/96/37.1
							2	466	MelRoV1-P2/4e-23/54/28.9
							3	293	MelRoV1-P3/2e-84/91/43.87
Purple Grass (<i>Pennisetum violaceum</i>)	monocot/ <i>Poaceae</i>	Pennisetum virus 1/ PenV1	PRJNA282366/ Suja George, M.S Swaminathan Research Foundation, India	RNA1/44.59X RNA2/112.25X	6284 3407	BK061790 BK061791	L	2033	LoPV1-L/0.0/98/51.27
							N	451	LoPV1-N/5e-79/75/40.52
							2	286	no hits
							3	151	LoPV1-P3/4e-12/83/30.16
Qinghai spruce (<i>Picea crassifolia</i>)	Gymnosperm/ <i>Pinaceae</i>	Picea virus 1/ PicV1	PRJNA307530/ [23]	RNA1/5.86X	11,193	BK061792	N	382	ASaV2-N/0.0/100/100
							2	452	ASaV2-P2/0.0/100/100
							3	318	ASaV2-P3/0.0/100/100
							4	174	ASaV2-P4/0.0/100/100
Jack pine (<i>Pinus banksiana</i>)	Gymnosperm/ <i>Pinaceae</i>	<i>Pinus banksiana</i> virus 1/ PiBanV1	PRJNA524866/ [45]	RNA1/97.66X	11276	BK061793	L	2051	PiFleV1-L/0.0/99/49.12
							N	406	PiFleV1-N/0.0/100/68.72
							2	433	PiFleV1-P2/3e-48/57/39.2
							3	317	PiFleV1-P3/1e-161/100/64.78
Yunnan pine (<i>Pinus yunnanensis</i>)	Gymnosperm/ <i>Pinaceae</i>	<i>Pinus yunnanensis</i> virus 1/PiYunV1	PRJNA507489/ [46]	RNA1/36.47X	12,057	BK061794	4	175	PiFleV1-P4/3e-17/65/36.84
							L	2048	PiFleV1-L/0.0/99/65.35
							N	411	PiFleV1-N/0.0/93/70.5
							2	440	PiFleV1-P2/7e-48/97/35.49
Spendlor primrose (<i>Primula oreodoxa</i>)	dicot/ <i>Primulaceae</i>	Primula virus 1/ PriV1	PRJNA544868/ [47]	RNA1/7.72X RNA2/149.23X	6352 6283	BK061795 BK061796	3	319	PiFleV1-P3/8e-145/100/62.38
							4	204	PiFleV1-P4/7e-30/75/38.46
							L	2048	PiFleV1-L/0.0/98/70.33
							N	2022	TfVV-L/0.0/98/42.3
							2	435	TfVV-N/1e-40/74/33.33
Goldilocks buttercup (<i>Ranunculus auricomus</i>)	dicot/ <i>Ranunculaceae</i>	Ranunculus virus 1/ RanV1	PRJNA217403/ [48]	RNA1/29.64X RNA2/163.27X	6481 6269	BK061797 BK061798	3	288	TfVV-P3/2e-28/75/29.55
							2	438	no hits
							3	307	ZaVV1-P3/2e-59/79/42.86
							4	200	no hits
							5	330	no hits
Radish (<i>Raphanus sativus</i>)	dicot/ <i>Brassicaceae</i>	Raphanus virus 1/ RapV1	PRJNA539856/ [49]	RNA1/165.02X RNA2/521.73X	6410 4144	BK061799 BK061800	L	2016	BrRV1-L/0.0/99/68.31
							N	439	BrRV1-N/1e-135/100/46.94
							2	411	BrRV1-P2/5e-14/61/28.57
Siberian currant (<i>Ribes diacanthum</i>)	dicot/ <i>Grossulariaceae</i>	Ribes virus 1/ RibV1	PRJNA407394/ [50]	RNA1/6.29X RNA2/33.97X	6323 5201	BK061801 BK061802	3	301	BrRV1-P3/6e-34/98/37.5
							L	2017	SpV1-L/0.0/98/47.29
							N	372	TfVV-N/1e-60/90/36.01no hits
							2	402	TfVV-P3/2e-45/82/33.33
							4	194	no hits

Table 1. Cont.

Plant Host	Taxa/Family	Virus Name/Abbreviation	Bioproject ID/Data Citation	Segment/Coverage	Length (nt)	Accession Number	Protein ID	Length (aa)	Highest Scoring Virus-Protein/E-Value/Query Coverage%/Identity% (Blast P)
Japanese umbrella pine (<i>Sciadopitys verticillata</i>)	Gymnosperm/ <i>Sciadopityaceae</i>	Sciadopitys virus 1_Chi/ SciV1_Chi	PRJNA396655/ Institute of Botany, CAS, China	RNA1/98.99X	11,224	BK061803	N	389	ASaV2-N/1e-111/95/43.13
							2	466	ASaV2-P2/1e-22/60/30.14
							3	315	ASaV2-P3/4e-104/95/48.23
							4	168	PiFleV1-P4/3e-05/67/26.32
L	2054	PiFleV1-L/0.0/99/46.13							
Japanese umbrella pine (<i>Sciadopitys verticillata</i>)	Gymnosperm/ <i>Sciadopityaceae</i>	Sciadopitys virus 1_Can/ SciV1_Can	PRJEB4921/ [51]	RNA1/14.02X	11,132	BK061804	N	389	ASaV2-N/1e-111/95/43.67
							2	466	ASaV2-P2/8e-22/60/29.87
							3	314	ASaV2-P3/2e-105/95/48.23
							4	168	PiFleV1-P4/7e-07/80/25.93
L	2071	PiFleV1-L/0.0/99/45.88							
Woolly grassland senecio (<i>Senecio coronatus</i>)	dicot/ <i>Asteraceae</i>	Senecio virus 1/ SenV1	PRJNA312157/ [52]	RNA1/10.59X RNA2/93.61X	6173 * 5617	BK061805 BK061806	L	2031 *	LBVaV-L/0.0/98/42.8
							N	376	PhPV1/2e-132/98/51.98
							2	345	no hits
							3	294	PhPV1-P3/9e-124/87/56.64
							4	147	no hits
5	370	XVV-L/2e-08/29/30							
Bladder campion (<i>Silene vulgaris</i>)	dicot/ <i>Caryophyllaceae</i>	Silene virus 1/ SilV1	PRJNA104951/ [53]	RNA1/29.59X RNA2/77.05X	6391 4363	BK061807 BK061808	L	2019	SpV1-0.0/99/59.91
							N	445	SpV1-N/4e-65/91/33.99
							2	509	SpV1-P2/2e-13/61/24.07
							3	179	BrRV1-P3/0.001/97/24.29
Broadhead daisy (<i>Streptoglossa macrocephala</i>)	dicot/ <i>Asteraceae</i>	Streptoglossa virus 1/ StrV1	PRJNA371565/ [28]	RNA1/131.33X RNA2/140.03X	6776 5130	BK061813 BK061814	L	2023	LoPV1-L/0.0/99/49.09
							N	449	InPRV-N3e-86/99/36.01
							2	333	no hits
							3	287	PhPV1-P3/2e-43/91/32.2
4	162	no hits							
Tansy (<i>Tanacetum vulgare</i>)	dicot/ <i>Asteraceae</i>	Tanacetum virus 1/ TanV1	PRJNA646340/ [54]	RNA1/10.19X RNA2/239.11X	6888 4608	BK061815 BK061816	L	2020	BrRV1-L/0.0/98/49.03
							N	447	BrRV1-L/8e-52/88/30.56
							2	505	no hits
3	176	RCaVV-P3/3e-05/73/30.60							
Hybrid yew (<i>Taxus media</i>)	Gymnosperm/ <i>Taxaceae</i>	Taxus virus 1/ TaxV1	PRJNA497542/ [55]	RNA1/57.28X	11,174	BK061817	N	382	ASaV2-N/7e-111/96/43.55
							2	417	ASaV2-P2/1e-18/68/26.28
							3	310	ASaV2-P3/3e-94/93/45.25
							4	201	no hits
							L	2057	PiFleV1-L/0.0/98/46.81
Chinese nutmeg yew (<i>Torreya grandis</i>)	Gymnosperm/ <i>Taxaceae</i>	Torreya virus 1/ TorV1	PRJNA498605 [25]	RNA1/59.04X	10,253	BK061818	N	379	TfVV-N/2e-57/93/32.5
							2	339	no hits
							3	283	TfVV-P3/4e-28/67/36.27
							4	152	no hits
L	2002	TfVV-L/0.0/97/35.4							
Liverwort (<i>Treubia lacunosa</i>)	Marchantiophyta/ <i>Treubiaceae</i>	Treubia virus 1/ TreV1	PRJNA505755/ Fairylake Botanical Garden, China	RNA1/364.20X RNA2/350.53X	6684 4940	BK061819 BK061820	L	2040	TfVV-L/0.0/99/54.2
							N	392	TfVV-N/3e-116/99/46.27
							2	395	TfVV-P2/0.015/56/24.34
							3	288	TfVV-P3/1e-114/85/55.07
4	153	no hits							
Wheat (<i>Triticum aestivum</i>)	monocot/ <i>Poaceae</i>	Triticum virus 1/ TriV1	PRJNA558380/ [56]	RNA1/10.25X RNA2/16.64X	6290 4103	BK061821 BK061822	L	2019	RCaVV-L/0.0/99/72.58
							N	430	RCaVV-N/8e-135/99/46.26
							2	451	RCaVV-P2/2e-32/67/30.70
3	179	RCaVV-P3/1e-48/100/44.13							
Variegated swallow-wort (<i>Vincetoxicum versicolor</i>)	dicot/ <i>Apocynaceae</i>	Vincetoxicum virus 1/ VinV1	PRJNA599262/ [57]	RNA1/56.05X RNA2/140.76X	6598 4655	BK061823 BK061824	L	2037	MelRoV1-L/0.0/99/48.19
							N	430	ZaVV1-N/7e-63/76/35
							2	356	MelRoV1-P2/2e-08/68/21.15
							3	307	MelRoV1-P3/63.51/80/36.44
4	174	no hits							
Corn (<i>Zea mays</i>)	monocot/ <i>Poaceae</i>	Zea virus 1/ ZeaV1	PRJNA407369/ [58]	RNA1/6.25X RNA2/40.88X	6345 4607	BK061825 BK061826	L	2037	AMVV1-L/0.0/99/49.07
							N	483	AMVV1-N/2e-90/76/40.92
							2	353	LoPV1-P2/4e-08/63/24.89
							3	286	TfVV-P3/6e-48/94/31.11
4	158	LoPV1-P3/1e-09/86/29.2							

* partial sequence.

2.3. Bioinformatics Tools and Analyses

2.3.1. Sequence Analyses

ORFs were predicted with ORFfinder (minimal ORF length 150 nt, genetic code 1, <https://www.ncbi.nlm.nih.gov/orffinder/>, accessed on 22 August 2022) and the functional domains and architectures of translated gene products were determined using InterPro (<https://www.ebi.ac.uk/interpro/search/sequence-search>, accessed on 22 August 2022)

and the NCBI conserved domain database-CDD v3.19 (<https://www.ncbi.nlm.nih.gov/Structure/cdd/wrpsb.cgi>, accessed on 22 August 2022). Further, HHPred and HHBlits, as implemented in <https://toolkit.tuebingen.mpg.de/#/tools/> (accessed on 22 August 2022), were used to complement the annotation of divergent predicted proteins by hidden Markov models. Transmembrane domains were predicted using the TMHMM version 2.0 tool (<http://www.cbs.dtu.dk/services/TMHMM/>, accessed on 22 August 2022).

2.3.2. Pairwise Sequence Identity

Percentage amino acid (aa) sequence identities of the L protein of those varicosaviruses identified in this study, as well as those available in the NCBI database, were calculated using SDTv1.2 [59]. Virus names, abbreviations, and NCBI accession numbers of the varicosaviruses already reported are shown in Supplementary Table S1.

2.3.3. Phylogenetic Analysis

Phylogenetic analysis based on the predicted polymerase protein of all available varicosaviruses was completed using MAFFT 7.505 (<https://mafft.cbrc.jp/alignment/software>) (accessed on 25 August 2022) with multiple aa sequence alignments and using FFT-NS-i as the best-fit model. The aligned aa sequences were used as inputs to generate phylogenetic trees using the maximum-likelihood method (best-fit model = E-INS-i) with the FastTree 2.1.11 tool (available at <http://www.microbesonline.org/fasttree/>) (accessed on 25 August 2022). Local support values were calculated with the Shimodaira-Hasegawa test (SH) and 1000 trees were resampled. The L proteins of four selected cytorhabdoviruses were used as outgroups. To explore the potential phylogenetic co-divergence of varicosaviruses with their associated host plants, plant host cladograms were generated in phyloT v.2 (<https://phyloT.biobyte.de/>, accessed on 26 August 2022) based on NCBI Taxonomy. Connections were manually inferred between the viral and plant phylograms and cladograms and visually inspected.

3. Results and Discussion

Most varicosaviruses likely do not induce easily discernable disease symptoms. Since their presence is not expected in the sequencing libraries of apparently “healthy” vegetables, they are ideal candidates to be identified through mining publicly available metatranscriptomic data. Accordingly, very recently, 12 novel proposed varicosaviruses were discovered when publicly available transcriptome datasets were mined [6,9,17,18]. Therefore, to unlock the hidden diversity of varicosaviruses, we extensively searched for these viruses in already available plant transcriptome data. This bioinformatics research resulted in the identification of 45 novel varicosaviruses, including the corrected full-length coding genome segments of the previously reported *Arceuthobium sichuanense*-associated virus 2 (ASaV2) [18], which had apparently been reconstructed from the genome segments of two different varicosaviruses. We also identified three novel variants of three recently discovered varicosaviruses, confirming and strengthening the results previously reported by Bejerman et al. [9]. This significant number of newly discovered varicosaviruses represents a 3.5-fold increase in the known varicosaviruses (Supplementary Figure S1), which clearly highlights the importance of data-driven virus discovery to illuminate the landscape of largely overlooked taxonomic groups, such as varicosaviruses.

More details, identification, assembly, and curation of raw SRA reads in this study resulted in 39 viral genome sequences with full-length coding regions and six with nearly complete coding regions. These viruses were associated with 45 plant host species (Table 1). Most of the tentative plant hosts of the novel varicosaviruses are herbaceous dicots (24/45), nine are herbaceous monocots, eight are gymnosperms, and four are liverworts and ferns (Table 1).

The genomes of 37 viruses identified in this study were bisegmented, where the RNA 1 of 36 of them encodes only the L protein, while the RNA 1 of *Chamaemelum virus 1* (ChaV1) has an additional ORF 5' to the L gene, supported by the identification of the conserved

intergenic sequence (see below), encoding a 171 aa putative protein (Table 1, Figure 1), which appears to be the first varicosavirus reported with an ORF in this position. The RNA 2 segments of these 37 viruses have three to five genes in the order 3'-N-PX-5'. Twelve of them have three genes, while 17 have four genes and eight contained five genes (Table 1, Figure 1). Of the previously reported varicosaviruses, six have three genes, four have four genes, and four have five genes; therefore, RNA 2 has a flexible genomic architecture and is apparently the most frequent genomic organization in the RNA 2 of varicosaviruses that includes four genes (21 members) or three genes (18 members).

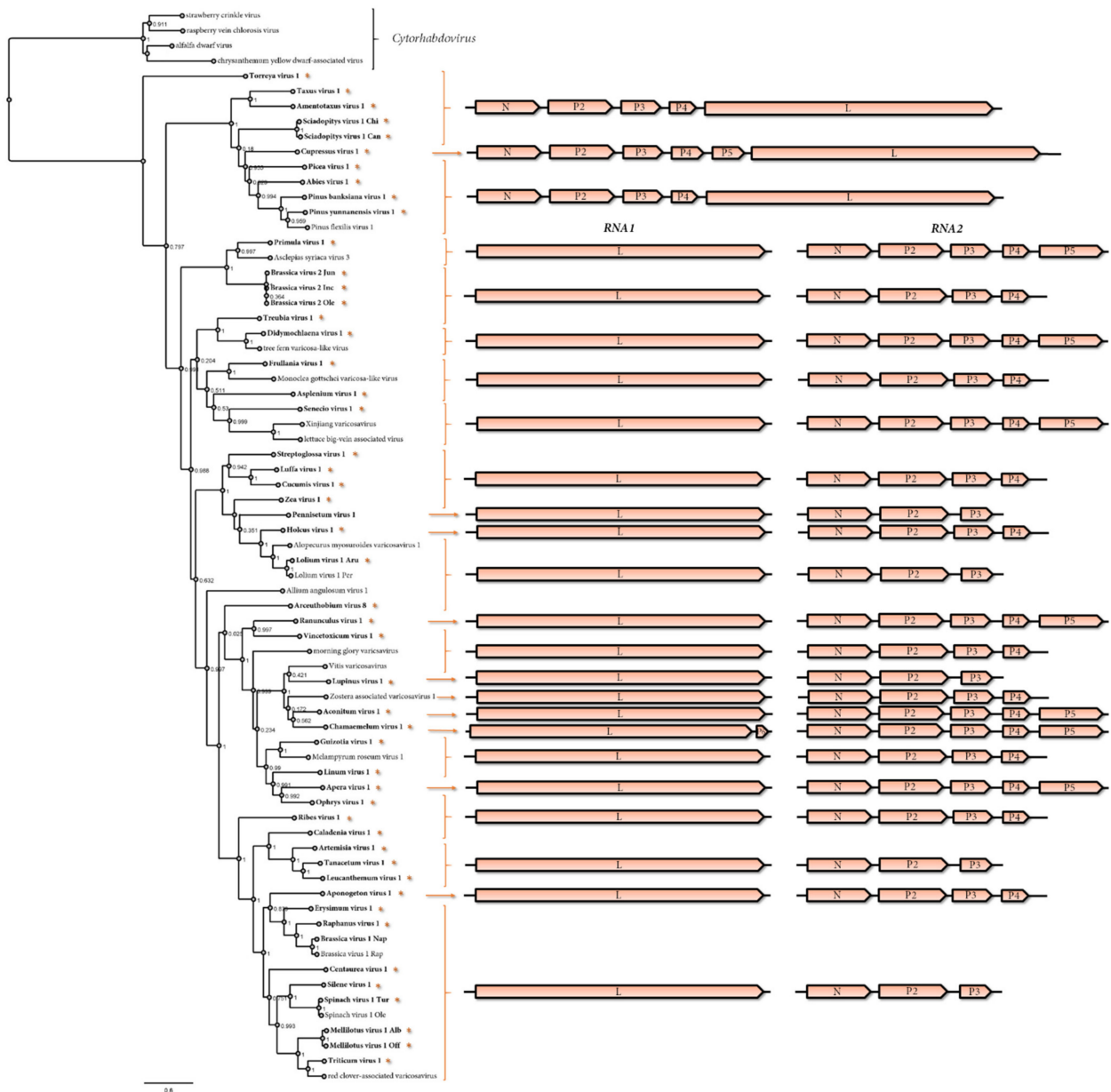


Figure 1. Left: Maximum-likelihood phylogenetic tree based on the amino acid sequence alignments of the complete L gene of all the varicosaviruses reported thus far and in this study. The scale bar indicates the number of substitutions per site. The node labels indicate fast tree support values. Four cytorhabdoviruses were used as outgroups. Right: Genomic organization of the varicosavirus sequences used in the phylogeny. An asterisk and bold font indicate those viruses identified in this study. The accession numbers of all the viruses are listed in Supplementary Table S1 and Table 1.

The consensus gene junction sequences of the bisegmented varicosaviruses were determined to be 3' AU(N)₅UUUUUGCUCU 5' (Table 2), while the gene junction sequences of all but one of the unsegmented varicosaviruses differed slightly in the 3' end, being GU(N)₅ instead of AU(N)₅ (Table 2). Strikingly, the consensus gene junction of the unsegmented Torreyia virus 1 (TorV1) was similar to that of the bisegmented varicosaviruses. The potential implication of this difference in the gene junctions needs to be explored since it could be linked to the basal evolutionary grouping of TorV1 (see below).

Table 2. Consensus varicosavirus gene junction sequences.

Virus *	3' end mRNA	Intergenic Spacer	5' end mRNA
AbiV1	CU(N) ₅ UUUUU	G	CUCU
ArcV8	AU(N) ₅ UUUUU	G	CUCU
AcoV1	AU(N) ₅ UUUUU	G	CUCU
AmeV1	CU(N) ₅ UUUUU	G	CUCU
ApeV1	AU(N) ₅ UUUUU	G	CUCU
ApoV1	AU(N) ₅ UUUUU	G	CUCU
ArtV1	AU(N) ₅ UUUUU	G	CUCU
AscSyV3	AU(N) ₅ UUUUU	G	CUCU
AspV1	AU(N) ₅ UUUUU	G	CUCU
BrV2	AU(N) ₅ UUUUU	G	CUCU
CalV1	AU(N) ₅ UUUUU	G	CUCU
CenV1	AU(N) ₅ UUUUU	G	CUCU
ChaV1	AU(N) ₅ UUUUU	G	CUCU
CucV1	AU(N) ₅ UUUUU	G	CUCU
CupV1	CU(N) ₅ UUUUU	G	CUCU
DidV1	AU(N) ₅ UUUUU	G	CUCU
EryV1	AU(N) ₅ UUUUU	G	CUCU
FruV1	AU(N) ₅ UUUUU	G	CUCU
GuiV1	AU(N) ₅ UUUUU	G	CUCU
HolV1	AU(N) ₅ UUUUU	G	CUCU
LeuV1	AU(N) ₅ UUUUU	G	CUCU
LinV1	AU(N) ₅ UUUUU	G	CUCU
LufV1	AU(N) ₅ UUUUU	G	CUCU
LupV1	AU(N) ₅ UUUUU	G	CUCU
MelV1	AU(N) ₅ UUUUU	G	CUCU
OphV1	AU(N) ₅ UUUUU	G	CUCU
PenV1	AU(N) ₅ UUUUU	G	CUCU
PicV1	CU(N) ₅ UUUUU	G	CUCU
PiBanV1	CU(N) ₅ UUUUU	G	CUCU
PiYunV1	CU(N) ₅ UUUUU	G	CUCU
PriV1	AU(N) ₅ UUUUU	G	CUCU
RanV1	AU(N) ₅ UUUUU	G	CUCU
RapV1	AU(N) ₅ UUUUU	G	CUCU
RibV1	AU(N) ₅ UUUUU	G	CUCU

Table 2. Cont.

Virus *	3' end mRNA	Intergenic Spacer	5' end mRNA
SciV1	CU(N) ₅ UUUUU	G	CUCU
SenV1	AU(N) ₅ UUUUU	G	CUCU
SilV1	AU(N) ₅ UUUUU	G	CUCU
StrV1	AU(N) ₅ UUUUU	G	CUCU
TanV1	AU(N) ₅ UUUUU	G	CUCU
TaxV1	CU(N) ₅ UUUUU	G	CUCU
TorV1	AU(N) ₅ UUUUU	G	CUCU
TreV1	AU(N) ₅ UUUUU	G	CUCU
TriV1	AU(N) ₅ UUUUU	G	CUCU
VinV1	AU(N) ₅ UUUUU	G	CUCU
ZeaV1	AU(N) ₅ UUUUU	G	CUCU
AAnV1	AU(N) ₅ UUUUU	G	CUCU
AMVV1	AU(N) ₅ UUUUU	G	CUCU
BrV1	AU(N) ₅ UUUUU	G	CUCA
LBVaV	AU(N) ₅ UUUUU	G	CUCU
LoV1	AU(N) ₅ UUUUU	G	CUCU
MelRoV1	AU(N) ₅ UUUUU	G	CUCU
MGVV	AU(N) ₅ UUUUU	G	CUCU
MgVV	AU(N) ₅ UUUUU	G	CUCU
PhPiV1	AU(N) ₅ UUUUU	G	CUCU
PiFleV1	GU(N) ₅ UUUUU	G	CUCU
RCaVV	AU(N) ₅ UUUUU	G	CUCU
SpV1	AU(N) ₅ UUUUU	G	CUCU
TfVV	AU(N) ₅ UUUUU	G	CUCU
VVV	AU(N) ₅ UUUUU	G	CUCU
XVV	AU(N) ₅ UUUUU	G	CUCU
ZaVV1	AU(N) ₅ UUUUU	G	CUCU

The consensus gene junction sequences of the viruses identified in this study are highlighted in light grey. * Names and abbreviations of newly identified viruses are listed in Table 1; while the names and abbreviations of known viruses are listed in Supplementary Table S1.

There is a great dearth of data on the potential functions of putative proteins, other than N and L, encoded by varicosaviruses, and, intriguingly, there were no conserved domains identified in these proteins. We grasped some shared identities, primarily for the cognate P3 (but also for several P2 proteins) (Table 1), though for most of the encoded proteins, the BlastP results were orphans, with no known signals or domains present and no clues towards their putative (or conserved) function. Thus, further studies should be focused on the functional characterization of these proteins to gain essential knowledge regarding the elusive proteome of varicosaviruses beyond the N and L proteins.

The pairwise aa sequence identities between the L proteins of all the reported varicosaviruses, including those identified in this study, showed great diversity and an overall low identity between the different varicosaviruses (Figure 2, Supplementary Table S2). Relatively low sequence identity is a common feature among rhabdovirus taxa, characterized by a high level of diversity in both the genome sequence and organization [10]. In addition, the overall low sequence identity among the novel viruses detected here and

with the previously described varicosaviruses suggests that despite the many viruses identified in this study, there likely remains a significant amount of virus “dark matter” for yet-to-be-discovered varicosaviruses.

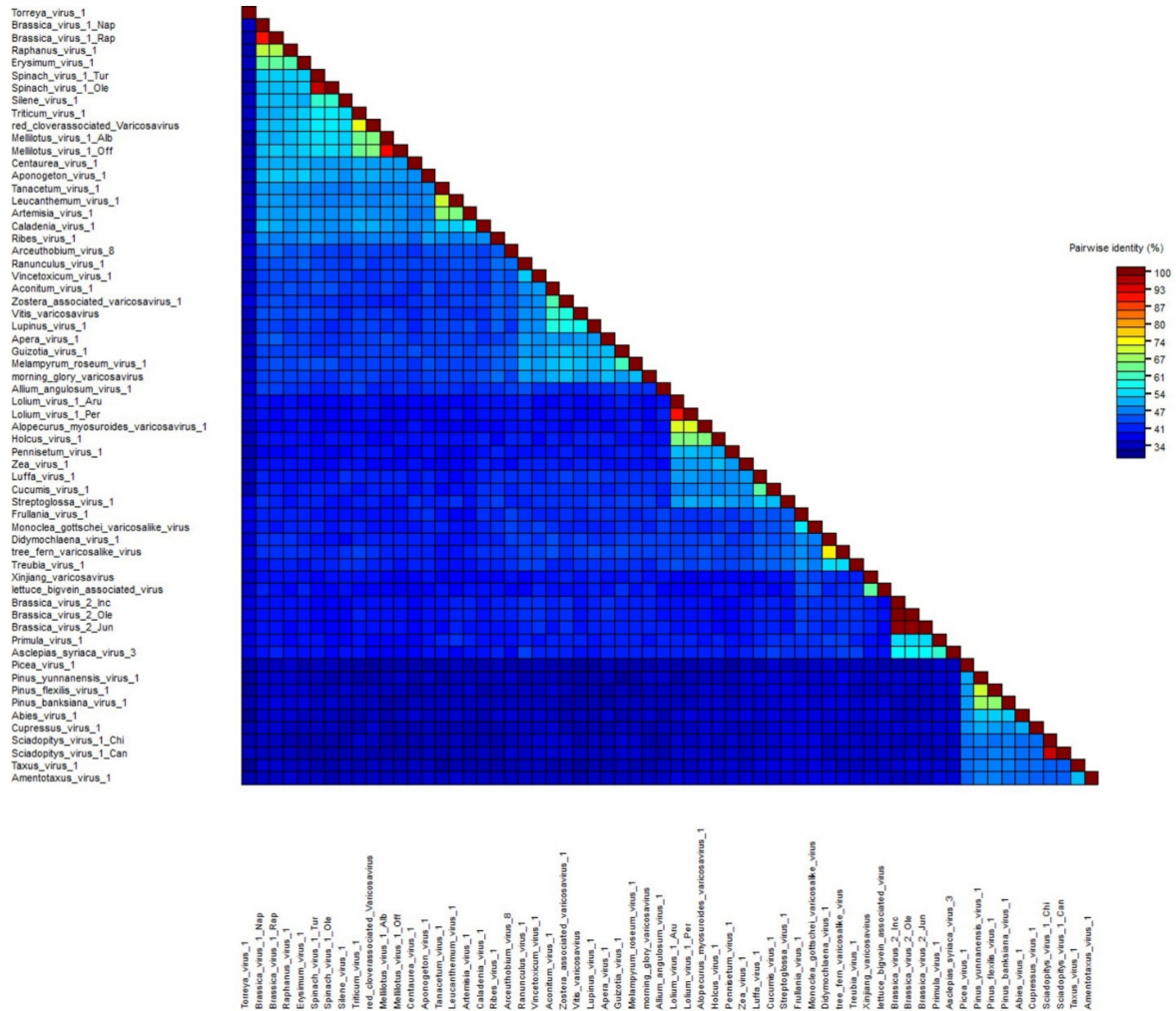


Figure 2. Pairwise identity matrix of the amino acid sequences of the varicosavirus complete L gene open reading frame generated using SDT v1.2 software [59]. GenBank accession numbers are listed in Supplementary Table S1 and Table 1.

When we analyzed the diversity between the variants of viruses which are likely members of the same species, we found that proteins encoded by the Brassica virus 2, Spinach virus 1, and Sciadopitysvirus 1 variants were very similar. On the other hand, proteins encoded by the Brassica virus 1, Lolium virus 1, and Melilotus virus 1 variants were quite diverse, but, nevertheless, they showed aa identities for the N and L proteins exceeding 80%. Thus, we tentatively propose an aa sequence identity of 80% across the L gene as the threshold for species demarcation in the *Varicosavirus* genus, a taxonomic criterion which had previously not been fully defined [10]. This threshold is strongly supported by the comparison of the L protein aa sequence of 60 viruses (Figure 2, Supplementary Table S2). Based on this criterion, all 39 novel viruses with their complete coding region assembled in this study should be considered as belonging to novel *Varicosavirus* species, which would increase the number of members of the genus by more than an order of magnitude.

Bejerman et al. [9] tentatively reported the first unsegmented varicosavirus, *Pinus flexilis virus 1* (PiFleV1), which was associated with the gymnosperm *Pinus flexilis*. In this study, we complemented that result by the discovery of eight additional unsegmented varicosaviruses which were exclusively associated with gymnosperms (Table 1), some of which

are linked to the same genus *Pinus* and present a significant co-evolution of viruses and hosts. These results robustly support a clade of gymnosperm-associated varicosaviruses with a distinct genome architecture, requiring the rewriting of a previously proposed key feature and fundamental marker of varicosaviruses: their genomic bisegmented nature. It is tempting to speculate that the unsegmented genomic architecture may be linked to the adaptation to gymnosperm hosts and a shared ancient evolutionary history of these viruses and hosts.

Interestingly, in the BlastP analyses of N, P2, and P3 of the gymnosperm-associated viruses, most of them had, as a best hit to the cognate proteins encoded by the putative bisegmented ASaV2 (Table 1), a virus apparently hosted by a parasitic plant of spruce (*Picea*, *Pinaceae*). Furthermore, unexpectedly, the best hit of the putative P5 protein encoded on ASaV2 RNA2 was a fragment of the PiFleV1 L protein, while the deduced L protein on ASaV2 RN1 was not a best hit with PiFleV1, but instead, with the non-gymnosperm-linked MelRoV1 hosted by the Orobanchaceae parasitic plant *Melampyrum roseum*. Thus, we suspected that ASaV2 was potentially misassembled from fragments belonging to two different viruses. Consequently, we re-analyzed the original SRA data used by Sidhartan et al. [18] and were able to assemble two distinct varicosavirus genomes: one bisegmented genome presumably linked to the parasitic plant and one unsegmented genome most likely linked to spruce, which would support our hypothesis. We believe that there are several reasons that led to the original ASaV2 description: (i) the atypical and unexpected existence at the time of an unsegmented varicosavirus; (ii) the presence of two varicosaviruses in the very same sequencing library, which may be the first tentative evidence in the literature of co-infection of two varicosaviruses; and (iii) the fact that the sequence reads corresponding to the L gene region of the unsegmented varicosavirus were low, which may have affected the assembling pipelines used by the authors. All in all, independently verifying unexpected re-analysed SRA data may lead to a clearer understanding of the genomic structure of the mined RNA virus genomes. Nevertheless, the inability to return to the original biological material to replicate, confirm, and validate the assembled viral genome sequences is a significant limitation of the data mining approach for virus discovery. Thus, researchers must be cautious when analysing SRA public data for virus discovery and understand the preliminary nature of its results.

The phylogenetic analysis based on the deduced L protein aa sequences placed all unsegmented varicosaviruses, except TorV1, into a distinct clade. Interestingly, TorV1 was placed in a clade that was basal to all varicosaviruses (Figure 1). This distinct phylogenetic branching and clustering of the unsegmented viruses suggests that they share a unique evolutionary history among varicosaviruses. Moreover, this may suggest that bisegmented varicosaviruses are evolutionarily younger than unsegmented ones. It may also mean that a genome split in varicosa-like viruses occurred after the radiation of gymnosperms and angiosperms. Bisegmented varicosaviruses did not cluster according to their genomic organization, nor did they cluster with the plant species associated with each virus (Figure 1). For example, brassica virus 1 and brassica virus 2 were placed in distinct clades, while two viruses associated with orchids (Ophius virus 1 and Caladenia virus 1) were placed in different clusters, and monocot-associated viruses were not all grouped together. On the other hand, all varicosaviruses associated with ferns and liverworts belonged to the same cluster, which was also shared with previously reported varicosaviruses from these plant types, while most of the grass-associated varicosaviruses were also clustered together (Figure 1).

We generated a tanglegram to compare the virus phylogram and plant host cladogram to further explore virus–host relationships (Figure 3). This analysis showed that the viruses of some clades clearly co-diverged with their hosts, including the gymnosperm-associated virus clade, the SpV1 and *Silene* virus 1 clade, the grass-associated virus clade, and the clade of fern and liverworts viruses, suggesting a shared host–virus evolution in those clades (Figure 3). However, the tanglegram topology also indicated that for most of the vari-

cosaviruses, there was no apparent concordant evolutionary history with their plant hosts, similar to what was previously reported for invertebrate and vertebrate rhabdoviruses [60].

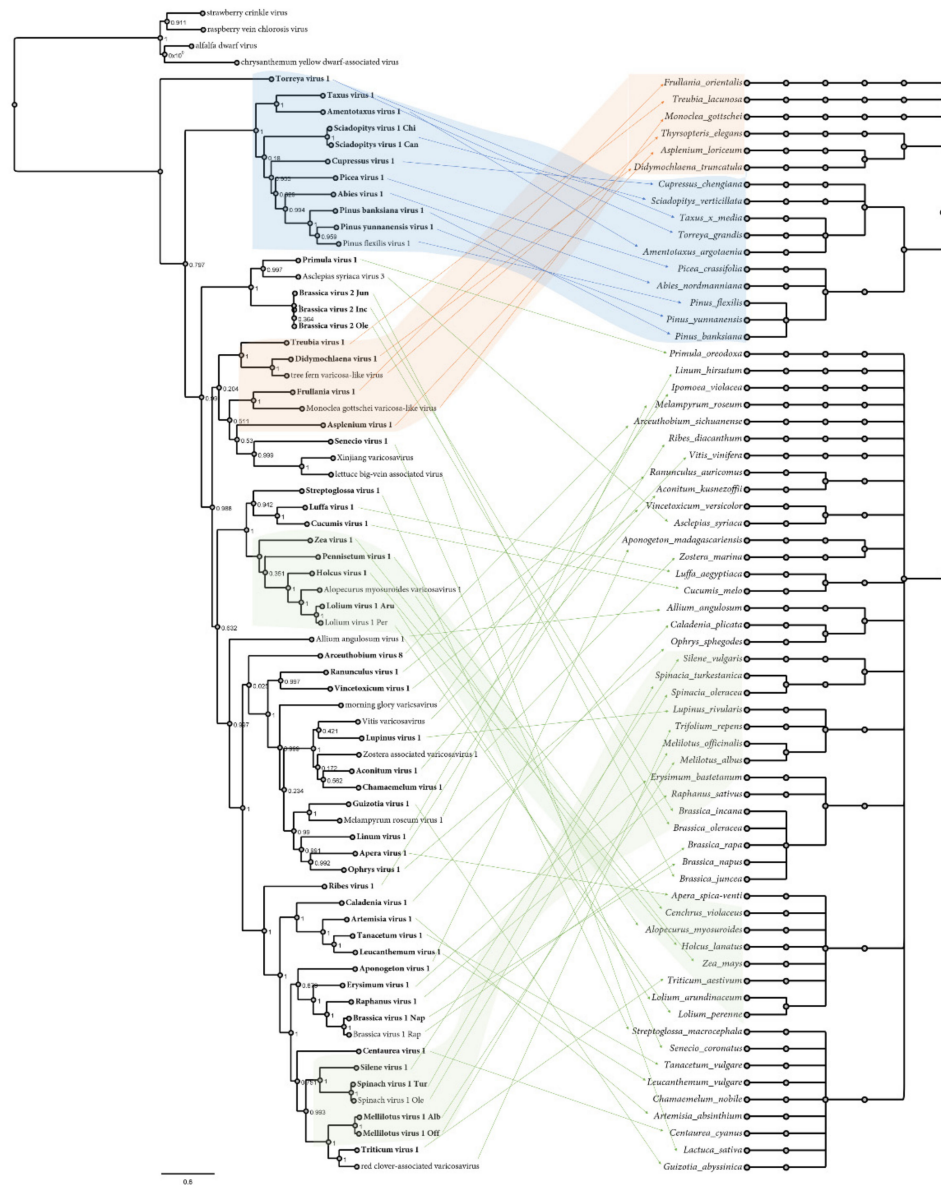


Figure 3. Tanglegram showing the phylogenetic relationships of the varicosaviruses (left), which are linked with the associated plant host(s) shown on the right. Links of well-supported clades of viruses to taxonomically related plant species are indicated in blue, orange, and green. A maximum likelihood phylogenetic tree of rhabdoviruses was constructed based on the conserved amino acid sequence of the complete L protein. Plant host cladograms were generated in phyloT v.2 based on NCBI taxonomy. Internal nodes represent the taxonomic structure of the NCBI taxonomy database, including species, genus, family, order, subclass, and sub-kingdom. Viruses identified in the present study are shown in bold font. The scale bar indicates the number of substitutions per site.

Several lines of evidence suggest that varicosaviruses may be vertically transmitted: (i) a close host–virus co-evolution in some clades may reflect species isolation and a lack of horizontal transmission, (ii) some viruses detected in this study were identified from seed transcriptomics databases, and (iii) an emerging characteristic of persistent, chronic infections of several plant viruses which are likely vertically transmitted are latent/asymptomatic infections, a characteristic which appears to be shared with varicosaviruses. Thus, further studies should be carried out to elucidate the transmission mode

of varicosaviruses beyond the fungal-transmitted LBVaV [11]. It is worth mentioning that even with the availability of thousands of RNAseq libraries of fungi and arthropods, we failed to detect any evidence of varicosaviruses in those organisms, which could suggest that vectors of varicosaviruses are rare or non-existent.

Before the era of data-driven virus discovery, few viruses had been identified in gymnosperms [61–64]. However, when data mining was applied to publicly available transcriptomes, many novel viruses were identified in this large group of higher plants, highlighting the rich and diverse gymnosperm virosphere, which still is largely unexplored. A distinct clade of gymnosperm-associated viruses was recently identified within amalgaviruses [65], while we recently described two distinct caulimovirids and geminivirids linked to the gnetophyte *Welwitschia mirabilis* [66]. Eight unsegmented varicosaviruses associated with gymnosperms were identified in this study, and another was discovered by Beijerman et al. [9]. Taken together, all of these recently discovered viruses in gymnosperms strongly suggest that they may have evolutionary trajectories that are distinct from those infecting angiosperms. Thus, it is likely that further exploration of additional gymnosperm datasets or new transcriptome studies of other gymnosperms will yield plenty of novel viruses with unique features, highlighting their close evolution with their hosts. The clear association between gymnosperm-associated viruses and their hosts likely indicates a close coevolution, which suggest an early adaptation of this group of viruses to infect gymnosperms. This hypothesis is also supported by the distinct genomic architecture and divergent evolutionary history among varicosaviruses, as shown in the phylogenetic tree, which are characterized by long branches and distinctive clustering. Taken together, the gymnosperm-associated varicosaviruses could be taxonomically classified in a novel genus within the family *Rhabdoviridae*, subfamily *Betarhabdovirinae*, for which we suggest the name “*Gymnorhavirus*”.

In summary, this study highlights the importance of the analysis of SRA public data as a valuable tool not only to accelerate the discovery of novel viruses, but also to gain insight into their evolution and to refine virus taxonomy. Using this approach, we looked for hidden varicosalike virus sequences to unlock the veiled diversity of a largely neglected plant rhabdovirus genus, the varicosaviruses. Our findings, including an approximately 3.5-fold expansion of the current genomic diversity within the genus, resulted in the most complete phylogeny of varicosaviruses to date, and they shed new light on the genomic architecture, phylogenetic relationships, and evolutionary landscape of this unique group of plant rhabdoviruses. Future studies should assess many intriguing aspects of the biology and ecology of these viruses such as potential symptoms, vertical transmission, and putative vectors.

Supplementary Materials: The following supporting information can be downloaded at: <https://www.mdpi.com/article/10.3390/pathogens11101127/s1>, Figure S1: Stacked bar chart showing the number of previously reported varicosaviruses and those in this study; Table S1: Virus names, abbreviations, and NCBI accession numbers of the varicosavirus sequences used in this study; Table S2: Amino acid sequence identity of the complete L gene ORF.

Author Contributions: Conceptualization, N.B., R.G.D. and H.D.; data analysis, N.B. and H.D.; writing—original draft preparation, N.B.; writing—review and editing, N.B., R.G.D. and H.D. All authors have read and agreed to the published version of the manuscript.

Funding: This research received no external funding. The participation of R.G.D. in this study was jointly supported by the Queensland Government Department of Agriculture and Fisheries and the University of Queensland through the Queensland Alliance for Agriculture and Food Innovation.

Institutional Review Board Statement: Not applicable.

Informed Consent Statement: Not applicable.

Data Availability Statement: The nucleotide sequence data reported are available in the Third Party Annotation Section of the DDBJ/ENA/GenBank databases under the accession numbers TPA: BK061731-BK061826. These sequences are available as Supplementary Materials.

Acknowledgments: The authors would like to express their sincere gratitude to the generators of the underlying data used for this work, which are cited in Table 1. By following open-access practices and supporting accessible raw sequence data in public repositories available to the research community, they have promoted the generation of new knowledge and ideas.

Conflicts of Interest: The authors declare no conflict of interest.

References

1. Koonin, E.V.; Krupovic, M.; Agol, V.I. The Baltimore Classification of Viruses 50 Years Later: How Does It Stand in the Light of Virus Evolution? *Microbiol. Mol. Biol. Rev.* **2021**, *85*, e0005321. [[CrossRef](#)]
2. Koonin, E.V.; Dolja, V.V.; Krupovic, M.; Varsani, A.; Wolf, Y.I.; Yutin, N.; Zerbini, F.M.; Kuhn, J.H. Global Organization and Proposed Megataxonomy of the Virus World. *Microbiol. Mol. Biol. Rev.* **2020**, *84*, e00061-19. [[CrossRef](#)] [[PubMed](#)]
3. Geoghegan, J.L.; Holmes, E.C. Predicting virus emergence amid evolutionary noise. *Open Biol.* **2017**, *7*, 170–189. [[CrossRef](#)] [[PubMed](#)]
4. Dolja, V.V.; Krupovic, M.; Koonin, E.V. Deep Roots and Splendid Boughs of the Global Plant Virome. *Annu. Rev. Phytopathol.* **2020**, *58*, 23–53. [[CrossRef](#)] [[PubMed](#)]
5. Edgar, R.C.; Taylor, J.; Lin, V.; Altman, T.; Barbera, P.; Meleshko, D.; Lohr, D.; Novakovsky, G.; Buchfink, B.; Al-Shayeb, B.; et al. Petabase-scale sequence alignment catalyses viral discovery. *Nature* **2022**, *602*, 142–147. [[CrossRef](#)]
6. Mifsud, J.C.O.; Gallagher, R.V.; Holmes, E.C.; Geoghegan, J.L. Transcriptome Mining Expands Knowledge of RNA Viruses across the Plant Kingdom. *J. Virol.* **2022**, e00260-22. [[CrossRef](#)]
7. Lauber, C.; Seitz, S. Opportunities and Challenges of Data-Driven Virus Discovery. *Biomolecules* **2022**, *12*, 1073. [[CrossRef](#)]
8. Dietzgen, R.G.; Bejerman, N.E.; Goodin, M.M.; Higgins, C.M.; Huot, O.B.; Kondo, H.; Martin, K.M.; Whitfield, A.E. Diversity and epidemiology of plant rhabdoviruses. *Virus Res.* **2020**, *281*, 197942. [[CrossRef](#)]
9. Bejerman, N.; Dietzgen, R.; Debat, H. Illuminating the Plant Rhabdovirus Landscape through Metatranscriptomics Data. *Viruses* **2021**, *13*, 1304. [[CrossRef](#)]
10. Walker, P.J.; Freitas-Astúa, J.; Bejerman, N.; Blasdel, K.R.; Breyta, R.; Dietzgen, R.G.; Fooks, A.R.; Kondo, H.; Kurath, G.; Kuzmin, I.V.; et al. ICTV Virus Taxonomy Profile: Rhabdoviridae 2022. *J. Gen. Virol.* **2022**, *103*, 001689. [[CrossRef](#)]
11. Campbell, R.N. Fungal Transmission of Plant Viruses. *Annu. Rev. Phytopathol.* **1996**, *34*, 87–108. [[CrossRef](#)] [[PubMed](#)]
12. Sasaya, T.; Ishikawa, K.; Koganezawa, H. The nucleotide sequence of RNA1 of Lettuce big-vein virus, genus Varicosavirus, reveals its relation to nonsegmented negative-strand RNA viruses. *Virology* **2002**, *297*, 289–297. [[CrossRef](#)] [[PubMed](#)]
13. Sasaya, T.; Kusaba, S.; Ishikawa, K.; Koganezawa, H. Nucleotide sequence of RNA2 of Lettuce big-vein virus and evidence for a possible transcription termination/initiation strategy similar to that of rhabdoviruses. *J. Gen. Virol.* **2004**, *85*, 2709–2717. [[CrossRef](#)]
14. Verbeek, M.; Dullemans, A.M.; van Bekkum, P.J.; van der Vlugt, R.A.A. Evidence for Lettuce big-vein associated virus as the causal agent of a syndrome of necrotic rings and spots in lettuce. *Plant Pathol.* **2013**, *62*, 444–451. [[CrossRef](#)]
15. Koloniuk, I.; Fránová, J.; Sarkisova, T.; Přibylková, J.; Lenz, O.; Petrzik, K.; Špak, J. Identification and molecular characterization of a novel varicosa-like virus from red clover. *Arch. Virol.* **2018**, *163*, 2213–2218. [[CrossRef](#)] [[PubMed](#)]
16. Sabbadin, F.; Glover, R.; Stafford, R.; Rozado-Aguirre, Z.; Boonham, N.; Adams, I.; Mumford, R.; Edwards, R. Transcriptome sequencing identifies novel persistent viruses in herbicide resistant wild-grasses. *Sci. Rep.* **2017**, *7*, srep41987. [[CrossRef](#)]
17. Shin, C.; Choi, D.; Hahn, Y. Identification of the genome sequence of Zostera associated varicosavirus 1, a novel negative-sense RNA virus, in the common eelgrass (*Zostera marina*) transcriptome. *Acta Virol.* **2022**, *65*, 373–380. [[CrossRef](#)]
18. Sidharthan, V.K.; Chaturvedi, K.K.; Baranwal, V.K. Diverse RNA viruses in a parasitic oowering plant (spruce dwarf mistletoe) revealed through RNA-seq data mining. *J. Gen. Plant Pathol.* **2022**, *88*, 138–144. [[CrossRef](#)]
19. Chen, Y.-M.; Sadiq, S.; Tian, J.-H.; Chen, X.; Lin, X.-D.; Shen, J.-J.; Chen, H.; Hao, Z.-Y.; Wille, M.; Zhou, Z.-C.; et al. RNA viromes from terrestrial sites across China expand environmental viral diversity. *Nat. Microbiol.* **2022**, *7*, 1312–1323. [[CrossRef](#)]
20. Nabeshima, T.; Abe, J. High-throughput sequencing indicates novel Varicosavirus, Emaravirus and Deltapartitvirus infections in *Vitis coignetiae*. *Viruses* **2021**, *13*, 827. [[CrossRef](#)]
21. Zhao, F.; Liu, H.; Qiao, Q.; Wang, Y.; Zhang, D.; Wang, S.; Tian, Y.; Zhang, Z. Complete genome sequence of a novel varicosavirus infecting tall morning glory (*Ipomoea purpurea*). *Arch. Virol.* **2021**, *166*, 3225–3228. [[CrossRef](#)]
22. Leebens-Mack, J.H.; Barker, M.S.; Carpenter, E.J. One thousand plant transcriptomes and the phylogenomics of green plants. *Nature* **2019**, *574*, 679–685.
23. Wang, Y.; Li, X.; Zhou, W.; Li, T.; Tian, C. De novo assembly and transcriptome characterization of spruce dwarf mistletoe *Arceuthobium sichuanense* uncovers gene expression profiling associated with plant development. *BMC Genom.* **2016**, *17*, 771. [[CrossRef](#)] [[PubMed](#)]
24. Tang, M.; Zhao, W.; Xing, M.; Zhao, J.; Jiang, Z.; You, J.; Ni, B.; Ni, Y.; Liu, C.; Li, J. Resource allocation strategies among vegetative growth, sexual reproduction, asexual reproduction and defense during growing season of *Aconitum kusnezoffii* Reichb. *Plant J.* **2021**, *105*, 957–977. [[CrossRef](#)]
25. Yu, C.; Zhan, X.; Zhang, C.; Xu, X.; Huang, J.; Feng, S.; Shen, C.; Wang, H. Comparative metabolomic analyses revealed the differential accumulation of taxoids, flavonoids and hormones among six Taxaceae trees. *Sci. Hortic.* **2021**, *285*, 110196. [[CrossRef](#)]

26. Babineau, M.; Mahmood, K.; Mathiassen, S.K.; Kudsk, P.; Kristensen, M. De novo transcriptome assembly analysis of weed *Apera spica-venti* from seven tissues and growth stages. *BMC Genom.* **2017**, *18*, 128. [[CrossRef](#)] [[PubMed](#)]
27. Rowarth, N.M.; Curtis, B.A.; Einfeldt, A.L.; Archibald, J.M.; Lacroix, C.R.; Gunawardena, A.H. RNA-Seq analysis reveals potential regulators of programmed cell death and leaf remodelling in lace plant (*Aponogeton madagascariensis*). *BMC Plant Biol.* **2021**, *21*, 375. [[CrossRef](#)] [[PubMed](#)]
28. Jayasena, A.S.; Fisher, M.F.; Panero, J.L.; Secco, D.; Bernath-Levin, K.; Berkowitz, O.; Taylor, N.L.; Schilling, E.E.; Whelan, J.; Mylne, J.S. Stepwise Evolution of a Buried Inhibitor Peptide over 45 My. *Mol. Biol. Evol.* **2017**, *34*, 1505–1516. [[CrossRef](#)]
29. Weitemier, K.; Straub, S.C.; Fishbein, M.; Bailey, C.D.; Cronn, R.C.; Liston, A. A draft genome and transcriptome of common milkweed (*Asclepias syriaca*) as resources for evolutionary, ecological, and molecular studies in milkweeds and Apocynaceae. *PeerJ* **2019**, *7*, e7649. [[CrossRef](#)]
30. Shen, H.; Jin, D.; Shu, J.-P.; Zhou, X.-L.; Lei, M.; Wei, R.; Shang, H.; Wei, H.-J.; Zhang, R.; Liu, L.; et al. Large-scale phylogenomic analysis resolves a backbone phylogeny in ferns. *GigaScience* **2017**, *7*, gix116. [[CrossRef](#)]
31. An, H.; Qi, X.; Gaynor, M.L.; Hao, Y.; Gebken, S.C.; Mabry, M.E.; McAlvay, A.C.; Teakle, G.R.; Conant, G.C.; Barker, M.S.; et al. Transcriptome and organellar sequencing highlights the complex origin and diversification of allotetraploid *Brassica napus*. *Nat. Commun.* **2019**, *10*, 2878. [[CrossRef](#)]
32. Bisht, D.S.; Chamola, R.; Nath, M.; Bhat, S.R. Molecular mapping of fertility restorer gene of an alloplasmic CMS system in *Brassica juncea* containing *Moricaandia arvensis* cytoplasm. *Mol. Breed.* **2015**, *35*, 14. [[CrossRef](#)]
33. Wu, Q.; Wang, J.; Mao, S.; Xu, H.; Wu, Q.; Liang, M.; Yuan, Y.; Liu, M.; Huang, K. Comparative transcriptome analyses of genes involved in sulfuraphane metabolism at different treatment in Chinese kale using full-length transcriptome sequencing. *BMC Genom.* **2019**, *20*, 377. [[CrossRef](#)]
34. Xu, H.; Bohman, B.; Wong, D.C.J.; Rodriguez-Delgado, C.; Scaffidi, A.; Flematti, G.R.; Phillips, R.D.; Pichersky, E.; Peakall, R. Complex Sexual Deception in an Orchid Is Achieved by Co-opting Two Independent Biosynthetic Pathways for Pollinator Attraction. *Curr. Biol.* **2017**, *27*, 1867–1877.e5. [[CrossRef](#)] [[PubMed](#)]
35. Tai, Y.; Hou, X.; Liu, C.; Sun, J.; Guo, C.; Su, L.; Jiang, W.; Ling, C.; Wang, C.; Wang, H.; et al. Phytochemical and comparative transcriptome analyses reveal different regulatory mechanisms in the terpenoid biosynthesis pathways between *Matricaria recutita* L. and *Chamaemelum nobile* L. *BMC Genom.* **2020**, *21*, 169. [[CrossRef](#)]
36. Lü, P.; Yu, S.; Zhu, N.; Chen, Y.-R.; Zhou, B.; Pan, Y.; Tzeng, D.; Fabi, J.P.; Argyris, J.; Garcia-Mas, J.; et al. Genome encode analyses reveal the basis of convergent evolution of fleshy fruit ripening. *Nat. Plants* **2018**, *4*, 784–791. [[CrossRef](#)]
37. Li, J.; Milne, R.I.; Ru, D.; Miao, J.; Tao, W.; Zhang, L.; Xu, J.; Liu, J.; Mao, K. Allopatric divergence and hybridization within *Cupressus chengiana* (Cupressaceae), a threatened conifer in the northern Hengduan Mountains of western China. *Mol. Ecol.* **2020**, *29*, 1250–1266. [[CrossRef](#)]
38. Huang, C.; Qi, X.; Chen, D.; Qi, J.; Ma, H. Recurrent genome duplication events likely contributed to both the ancient and recent rise of ferns. *J. Integr. Plant Biol.* **2019**, *62*, 433–455. [[CrossRef](#)]
39. Osuna-Mascaró, C.; de Casas, R.R.; Gómez, J.M.; Loureiro, J.; Castro, S.; Landis, J.B.; Hopkins, R.; Perfectti, F. Hybridization and introgression are prevalent in Southern European *Erysimum* (Brassicaceae) species. *Ann. Bot.* **2022**. [[CrossRef](#)] [[PubMed](#)]
40. Young, E.; Carey, M.; Meharg, A.A.; Meharg, C. Microbiome and ecotypic adaptation of *Holcus lanatus* (L.) to extremes of its soil pH range, investigated through transcriptome sequencing. *Microbiome* **2018**, *6*, 48. [[CrossRef](#)]
41. Nevada, B.; Atchison, G.W.; Hughes, C.E.; Filatov, D.A. Widespread adaptive evolution during repeated evolutionary radiations in New World lupins. *Nat. Commun.* **2016**, *7*, 12384. [[CrossRef](#)]
42. Wu, F.; Duan, Z.; Xu, P.; Yan, Q.; Meng, M.; Cao, M.; Jones, C.S.; Zong, X.; Zhou, P.; Wang, Y.; et al. Genome and systems biology of *Melilotus albus* provides insights into coumarins biosynthesis. *Plant Biotechnol. J.* **2021**, *20*, 592–609. [[CrossRef](#)] [[PubMed](#)]
43. Huang, R.; Snedden, W.; DiCenzo, G. Reference nodule transcriptomes for *Melilotus officinalis* and *Medicago sativa* cv. Algonquin. *Grassl. Res.* **2022**, *6*, e408. [[CrossRef](#)]
44. Piñeiro Fernández, L.; Byers, K.J.R.P.; Cai, J.; Sedeek, K.E.M.; Kellenberger, R.T.; Russo, A.; Qi, W.; Aquino Fournier, C.; Schlüter, P.M. A Phylogenomic Analysis of the Floral Transcriptomes of Sexually Deceptive and Rewarding European Orchids, *Ophrys* and *Gymnadenia*. *Front. Plant Sci.* **2019**, *10*, 1553. [[CrossRef](#)]
45. Peery, R.M.; McAllister, C.H.; Cullingham, C.I.; Mahon, E.L.; Arango-Velez, A.; Cooke, J.E. Comparative genomics of the chitinase gene family in lodgepole and jack pines: Contrasting responses to biotic threats and landscape level investigation of genetic differentiation. *Botany* **2021**, *99*, 355–378. [[CrossRef](#)]
46. Cai, N.; Xu, Y.; Chen, S.; He, B.; Li, G.; Li, Y.; Duan, A. Variation in seed and seedling traits and their relations to geo-climatic factors among populations in Yunnan Pine (*Pinus yunnanensis*). *J. For. Res.* **2016**, *27*, 1009–1017. [[CrossRef](#)]
47. Zhao, Z.; Luo, Z.; Yuan, S.; Mei, L.; Zhang, D. Global transcriptome and gene co-expression network analyses on the development of distyly in *Primula oreodoxa*. *Heredity* **2019**, *123*, 784–794. [[CrossRef](#)] [[PubMed](#)]
48. Pellino, M.; Hojsgaard, D.; Schmutzer, T.; Scholz, U.; Hörandl, E.; Vogel, H.; Sharbel, T.F. Asexual genome evolution in the apomictic *Ranunculus auricomus* complex: Examining the effects of hybridization and mutation accumulation. *Mol. Ecol.* **2013**, *22*, 5908–5921.
49. Yang, Z.; Li, W.; Su, X.; Ge, P.; Zhou, Y.; Hao, Y.; Shu, H.; Gao, C.; Cheng, S.; Zhu, G.; et al. Early Response of Radish to Heat Stress by Strand-Specific Transcriptome and miRNA Analysis. *Int. J. Mol. Sci.* **2019**, *20*, 3321. [[CrossRef](#)]

50. Zhou, B.; Wang, J.; Lou, H.; Wang, H.; Xu, Q. Comparative transcriptome analysis of dioecious, unisexual floral development in *Ribes diacanthum* pall. *Gene* **2019**, *699*, 43–53. [[CrossRef](#)] [[PubMed](#)]
51. Wickett, N.J.; Mirarab, S.; Nguyen, N.; Warnow, T.; Carpenter, E.; Matasci, N.; Ayyampalayam, S.; Barker, M.S.; Burleigh, J.G.; Gitzendanner, M.A.; et al. Phylotranscriptomic analysis of the origin and early diversification of land plants. *Proc. Natl. Acad. Sci. USA* **2014**, *111*, E4859–E4868. [[CrossRef](#)] [[PubMed](#)]
52. Meier, S.K.; Adams, N.; Wolf, M.; Balkwill, K.; Muasya, A.M.; Gehring, C.A.; Bishop, J.M.; Ingle, R.A. Comparative RNA-seq analysis of nickel hyperaccumulating and non-accumulating populations of *Senecio coronatus* (Asteraceae). *Plant J.* **2018**, *95*, 1023–1038. [[CrossRef](#)]
53. Baloun, J.; Nevrtalova, E.; Kovacova, V.; Hudzieczek, V.; Čegan, R.; Vyskot, B.; Hobza, R. Characterization of the HMA7 gene and transcriptomic analysis of candidate genes for copper tolerance in two *Silene vulgaris* ecotypes. *J. Plant Physiol.* **2014**, *171*, 1188–1196. [[CrossRef](#)]
54. Clancy, M.V.; Haberer, G.; Jud, W.; Niederbacher, B.; Niederbacher, S.; Senft, M.; Zytynska, S.E.; Weisser, W.W.; Schnitzler, J.-P. Under fire-simultaneous volatilome and transcriptome analysis unravels fine-scale responses of tansy chemotypes to dual herbivore attack. *BMC Plant Biol.* **2020**, *20*, 551. [[CrossRef](#)] [[PubMed](#)]
55. Zhou, T.; Luo, X.; Yu, C.; Zhang, C.; Zhang, L.; Song, Y.B.; Dong, M.; Shen, C. Transcriptome analyses provide insights into the expression pattern and sequence similarity of several taxol biosynthesis-related genes in three *Taxus* species. *BMC Plant Biol.* **2019**, *19*, 33. [[CrossRef](#)] [[PubMed](#)]
56. Hodge, B.A.; Paul, P.A.; Stewart, L.R. Occurrence and High-Throughput Sequencing of Viruses in Ohio Wheat. *Plant Dis.* **2020**, *104*, 1789–1800. [[CrossRef](#)]
57. Yu, X.; Wang, W.; Yang, H.; Zhang, X.; Wang, D.; Tian, X. Transcriptome and comparative chloroplast genome analysis of *Vincetoxicum versicolor*: Insights into molecular evolution and phylogenetic implication. *Front. Genet.* **2021**, *12*, 602528. [[CrossRef](#)]
58. Lanver, D.; Müller, A.N.; Happel, P.; Schweizer, G.; Haas, F.B.; Franitza, M.; Pellegrin, C.; Reissmann, S.; Altmüller, J.; Rensing, S.A.; et al. The Biotrophic Development of *Ustilago maydis* Studied by RNA-Seq Analysis. *Plant Cell* **2018**, *30*, 300–323. [[CrossRef](#)]
59. Muhire, B.M.; Varsani, A.; Martin, D.P. SDT: A Virus Classification Tool Based on Pairwise Sequence Alignment and Identity Calculation. *PLoS ONE* **2014**, *9*, e108277. [[CrossRef](#)]
60. Geoghegan, J.L.; Duchêne, S.; Holmes, E.C. Comparative analysis estimates the relative frequencies of co-divergence and cross-species transmission within viral families. *PLoS Pathog.* **2017**, *13*, e1006215. [[CrossRef](#)]
61. Alvarez-Quinto, R.A.; Lockhart, B.E.L.; Fetzer, J.L.; Olszewski, E.N. Genomic characterization of cycad leaf necrosis virus, the first badnavirus identified in a gymnosperm. *Arch. Virol.* **2020**, *165*, 1671–1673. [[CrossRef](#)] [[PubMed](#)]
62. Koh, S.H.; Li, H.; Admiraal, R.; Jones, M.G.; Wylie, S. Catharanthus mosaic virus: A potyvirus from a gymnosperm, *Welwitschia mirabilis*. *Virus Res.* **2015**, *203*, 41–46. [[CrossRef](#)] [[PubMed](#)]
63. Han, S.S.; Karasev, A.V.; Ieki, H.; Iwanami, T. Nucleotide sequence and taxonomy of *Cycas necrotic stunt virus*. *Arch. Virol.* **2002**, *147*, 2207–2214. [[CrossRef](#)] [[PubMed](#)]
64. Rastrojo, A.; Núñez, A.; Moreno, D.A.; Alcamí, A. A New Putative Caulimoviridae Genus Discovered through Air Metagenomics. *Microbiol. Resour. Announc.* **2018**, *7*, e00955-18. [[CrossRef](#)]
65. Sidharthan, V.K.; Rajeswari, V.; Vanamala, G.; Baranwal, V.K. Revisiting the amalgaviral landscapes in plant transcriptomes expands the host range of plant amalgaviruses. *Available SSRN 4210265* **2022**. [[CrossRef](#)]
66. Debat, H.; Bejerman, N. A glimpse into the DNA virome of the unique “living fossil” *Welwitschia mirabilis*. *Gene* **2022**, *843*, 146806. [[CrossRef](#)]